O.V. PROKOPENKO

Faculty of Radio Physics, Electronics and Computer Systems,
Taras Shevchenko National University of Kyiv
(64/13, Volodymyrska Str., Kyiv 01601, Ukraine; e-mail: Oleksandr.Prokopenko@gmail.com)

PACS 85.75.-d, 07.57.Hm

MICROWAVE SIGNAL SOURCES BASED ON SPIN-TORQUE NANO-OSCILLATORS

The spin-transfer torque (STT) effect provides a new method of manipulating the magnetization in nano-scale objects. According to the STT effect, a bias dc current traversing magnetic multilayers can transfer angular magnetic moments from one layer to another, which can give rise to the microwave dynamics of magnetization in the layer. This phenomenon can be used to develop novel microwave signal sources (MSSs). In this work, we review the main research results on MSSs based on the STT effect obtained at Taras Shevchenko National University of Kyiv and its foreign collaborating institutions in the recent years.

K e y w o r d s: spin-transfer torque, spin-torque nano-oscillator, microwave signal source.

1. Introduction

In 2005, just after the defence of my PhD thesis concerning the electromagnetic theory of surface wave resonators and microwave devices based on them, I began to think about the subject of my future research. At this very moment, my PhD supervisor, Prof. Gennady A. Melkov, a well-known expert on magnetism, superconductivity, and their microwave applications, had suggested that I continue my work in the area of magnetism. It was quite a new research area for me, so I was hesitant. However, my doubts were rapidly dismissed, when Professor Academician of NASU Mykola G. Nakhodkin invited my supervisor and his scientific group (and me among other group members) to work on the grant he was going to obtain from the Ministry of Education and Science of Ukraine. The subject of the grant was nanophysics and nanoelectronics. So, in order to work on the grant, I had to do research on magnetic nano-systems. Thus, under a positive influence of M.G. Nakhodkin and G.A. Melkov, I decided to work in the area of nano-sized magnetic structures and their applications at microwaves.

In this paper, I review the principal analytical and numerical results involving the physics of multilayer nano-structures based on the spin-transfer torque (STT) effect and their possible applications as microwave signal sources (MSSs) obtained by my coauthors and me for the last four years. All of the results presented below (excluding the most recent papers published in 2014) were obtained within the scope of several grants on nanophysics and nanoelectronics supervised by Professor Academician of NASU M.G. Nakhodkin.

The paper has the following structure. In Section 2, the fundamentals of MSSs based on the STT effect are introduced. In Section 3, I consider the direct dipole microwave emission from a spin-torque nano-oscillator (STNO) and an oscillator array and evaluate a possibility to use this phenomenon for the development of unconventional dipole-radiation MSSs. In Section 4, I analyze the microwave magnetization dynamics in a dual-free-layer (DFL) STNO having high-frequency high-power microwave output and consider the application of such an STNO as a MSS. The general theory of MSSs based on a vortex-state STNO is presented in Section 5. Finally, the summary of the obtained results and the conclusions are presented in Section 6.

2. Basic Physics of Microwave Sources Based on the Spin-Transfer Torque

The STT effect in magnetic multilayers was theoretically predicted in [1, 2] and experimentally observed in [3–12]. It provides a new method of manipulation of the magnetization direction in nano-magnetic systems, which can lead to the magnetization switching [3], generation of microwave oscillations under the action of a dc electric current [4–11], and the spin torque diode effect [12], which can then be used

for the development of practical microwave detectors [13], as well as for quantitatively measuring STT [14]. Since the prediction in 1996, the STT effect is thoroughly studied and considered for many applications [15–17].

The effect of microwave generation in magnetic multilayers under the action of a dc electric current was measured experimentally in [4]. According to the effect, a spin-polarized electric dc current passing through a magnetized ferromagnetic layer can transfer its angular momentum to this layer, and, as a result, change the orientation of the magnetization vector in the layer. This phenomenon leads to the magnetization precession with the frequency close to the frequency of the ferromagnetic resonance (FMR) in the magnetic layer at relatively low amplitudes of the spin-polarized current and, therefore, to the microwave oscillations of the multilayer resistance due to the giant magnetoresistance (GMR) [5, 8, 16, 17] or tunneling magnetoresistance (TMR) [7, 10, 16, 17] (type of the observed effect depends on the multilayer structure and properties).

Magnetic multilayered structures are used for the development of active nano-scale microwave devices – STNOs (Fig. 1). Typical STNOs have at least two magnetic layers, so-called free magnetic layer (FL) and fixed or pinned magnetic layer (PL), and a nonmagnetic spacer situated between the magnetic layers. The magnetization of the PL has a fixed direction, which determines the direction of spin-polarization of the electric current traversing the structure. The other magnetic layer, the FL, is typically used as an analyzer of the angular momentum transferred to this layer by a current. The magnetization of the FL is not strictly fixed in space and can relatively freely precess under the action of an external signal. A thin metallic (e.g., Cu) or dielectric (e.g., MgO) layer is used as a nonmagnetic spacer in STNOs based on GMR [5, 8, 16, 17] or TMR [7, 10, 16, 17] structures, respectively.

The STNO could be realized in two possible geometries [15–18]: magnetic nano-pillar or magnetic nano-contact (see Fig. 1). In the first case, the FL has finite lateral sizes in the plane of the layer, so the spin wave (SW) eigenmodes of the FL, which can be excited by the traversing spin-polarized current, have discrete frequencies determined by the finite in-plane sizes of the pillar [18]. In the other case of a nano-contact, the FL has the form of a magnetic film, and,
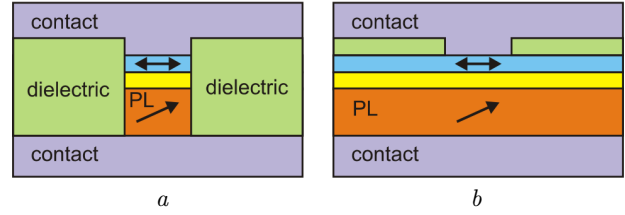

Fig. 1. Cross-section of two possible STNO geometries: (*a*) nano-pillar geometry and (*b*) nano-contact geometry. Double arrow indicates possible magnetization precession in the FL, normal arrow shows the magnetization direction in the PL

therefore, the magnetic oscillations excited by spin-polarized current, can excite propagating SW modes in the FL [18].

The typical STNO has the following geometrical parameters: radius of the structure $R \sim 10\text{–}10^3$ nm (for circular nano-pillars only), thickness of the FL $L \sim 1\text{–}10$ nm, thickness of the PL $L_p \sim 10\text{–}100$ nm, and spacer thickness $d \sim 1\text{–}10$ nm. The operation efficiency of the STNO strongly depends on the degree of spin polarization of the current, which is characterized by a dimensionless spin-polarization efficiency of the PL η. Typical values of η are about 0.2—0.5 for GMR STNOs and 0.5—0.7 for TMR junctions. The characteristic static resistance of an STNO R_{dc} can also vary in a wide range from $R_{dc} \sim 1\ \Omega$ for GMR STNOs to $R_{dc} \sim 1$ kΩ for TMR STNOs, respectively.

Although there are a lot of different theoretical approaches to the problem of microwave excitation of the FL by a spin-polarized electric current (for details, see [17, 18]), I briefly consider only a simple approximate analytic theory [18]. The model gives a clear simple physical picture of the nonlinear dynamical processes taking place in current-driven STNOs and can give an adequate description of most of the salient characteristics of real STNOs. The model equation for a dimensionless complex SW amplitude $c \equiv c(t)$ has the form [18]:

$$\frac{dc}{dt} + i\omega(p, I_{dc})c + \Gamma_+(p, I_{dc})c - \Gamma_-(p, I_{dc})c = 0, \quad (1)$$

where the term $i\omega(p, I_{dc})c$ describes a conservative magnetization precession in the FL, term $\Gamma_+(p, I_{dc})c$ characterizes damping of magnetization oscillations in the FL, and last term gives the effect of "negative" damping caused by the STT. Here, $p = |c|^2$, $i = \sqrt{-1}$, $\omega(p, I_{dc}) \approx \omega_0 + N_\omega p$ is the nonlinear angular frequency of magnetization precession, ω_0 is the

FMR frequency, N_ω is the nonlinear frequency shift $(\sim \omega_M)$, $\omega_M = \gamma \mu_0 M_0$, $\gamma = g \mu_B / \hbar \approx 2\pi \cdot 28$ GHz/T is the modulus of the gyromagnetic ratio, g is the spectroscopic Lande factor, μ_B is the Bohr magneton, $\hbar$ is the reduced Planck constant, μ_0 is the vacuum permeability, M_0 is the saturation magnetization of the FL, $\Gamma_+(p, I_{dc}) \approx \Gamma(1 + Yp)$ is the nonlinear "positive" damping coefficient in the system with natural damping rate $\Gamma = \alpha \omega_0$, α is the Gilbert damping parameter, $Y = 2\omega_M / \omega_0 - 1$ is the nonlinear damping parameter, $\Gamma_-(p, I_{dc}) \approx \sigma I_{dc}(1 - p)$ is the "negative" damping rate caused by the dc current I_{dc} traversing the structure, and σ is the current-torque coefficient.

The developed theory [18] in the case where the model parameters are known can be used to predict the behavior of an individual STNO (or an oscillator array) under the influence of an external dc signal. It is used below, in Section 5, when considering microwave oscillations in the vortex STNO.

3. Dipole-Radiation Microwave Signal Sources

The microwave power P_{MR} generated by a single STNO under the action of an applied dc current I_{dc} through the magnetoresistance (MR) mechanism can be evaluated as [19]: $P_{MR} \approx 0.5 I_{dc}^2 R_{dc} (R_{rf}/R_{dc})^2$, where R_{dc} and R_{rf} are the dc and microwave amplitudes of STNO resistance $R_{dc} + R_{rf} \cos(2\pi f t)$, respectively. In the case of an STNO based on the GMR [5, 8], this power is relatively small (around one nW), while, in the case of an STNO based on the TMR [7, 10], it can reach 1 μW.

The magnetization precession excited by a spin-polarized current in a FL of an STNO can manifest itself not only through the GMR and TMR effects. The precessing magnetization of the FL creates the oscillating dipolar magnetic field, which can be registered and channeled, if an appropriate microwave system is coupled to a generating STNO. The problem of the direct dipolar emission of a microwave signal generated by STNO in a free space has been considered in [20] and then thoroughly analyzed in [19]. It was found in [20] that the microwave signal directly emitted by STNO into a free space is substantially smaller than the signal that could be extracted from STNO through the MR effect. The situation, however, can be different if the emission takes place in a microwave transmission line or a resonator, or/and if an array of many phase-locked (or synchronized)

STNOs [9, 11, 21] placed in a microwave resonator is used to generate a microwave signal.

In our calculations, we used a simple model of direct microwave emission from a system of two effective magnetic dipoles developed in [20] with the expressions for the fields of a magnetic dipole from [20, 22] and the standard expressions for the electromagnetic fields of fundamental modes in the considered transmission lines and resonators [22]. We assumed that the magnetization of the FL is uniform (macrospin approximation) and that the sizes of the effective magnetic dipoles are much smaller than the wavelength λ of the microwave signal. In our calculations, we used the following typical parameters of STNO [7–10, 20]: $\mu_0 M_0 = 800$ mT, $R = 100$ nm, $L = 5$ nm, and the frequency of the magnetization precession $f = 10$ GHz. We also assumed that the permittivity ϵ and the permeability μ of a medium, where an STNO is placed, are approximately equal to the vacuum permittivity ϵ_0 and the vacuum permeability μ_0, respectively.

Using the above-described model, we obtained the following generalized expression for the microwave power emitted by a single STNO in an *arbitrary* microwave system [19]:

$$P_{dip}(f) = \frac{8}{3}\pi^3 P_0 \frac{V}{V_{eff}} Q \sin^2 \theta, \tag{2}$$

where $P_0 = \mu_0 M_0^2 V f$ is the characteristic microwave power emitted from the FL of an STNO, $V = \pi R^2 L$, V_{eff} is the effective volume of a particular microwave system coupled to STNO, Q is the quality factor of this system, and θ is the magnetization precession angle. The values of maximum microwave power (at $\theta = \pi/2$) emitted by a single STNO calculated for various systems are presented in Table along with the expressions for the effective volume V_{eff} for these systems.

The presented results demonstrate that, although the power emitted from an STNO into a free space is very low ($\sim 10^{-22}$ W), the coupling of an STNO to a microwave system can substantially increase the output power. In particular, if we place an STNO at the center of a gold nano-loop of the round shape with an inner radius of 10 μm and a square wire cross-section of 50×50 nm^2 having the characteristic resistance $R_L = 503$ Ω, we can increase the emitted power by approximately 10^{10} times, because the power can be collected by the loop in a near-field

Expressions for V_{eff} and values for maximum microwave power P_{dip} (at $\theta = \pi/2$)

Case	Expression for V_{eff}	Parameters	Maximum power, W
Free space	λ^3	$\lambda = 3$ cm, $Q = 1$	3.9×10^{-22}
Nano-loop	$4\pi R^2 R_{\text{L}}/3\mu_0 f$	$R_{\text{L}} = 503\ \Omega$, $Q = 1$	6.0×10^{-12}
Nano-sized square capacitor	$2\pi^3 \lambda^2 L^2 b/3a^2$	$a = 10\ \mu$m, $b = 50$ nm, $Q = 1$	1.1×10^{-11}
Rectangular waveguide	$16\pi a^2 b\chi/3$	$a = 23$ mm, $b = 50$ nm, $\chi = \zeta/\sqrt{1-\zeta^2}$, $\zeta = \lambda/2a \approx 0.65$, $Q = 1$	2.7×10^{-17}
Microstrip line	$64\pi ab\lambda/3$	$a = 10\ \mu$m, $b = 50$ nm, $Q = 1$	1.0×10^{-14}
Rectangular resonator	$4\pi^3 \lambda^2 b(1+\chi^2)^2/3\chi$	$a = 23$ mm, $b = 50$ nm, $Q = 10^5$	1.6×10^{-13}
Microstrip resonator	$16\pi^3 ab\lambda/3$	$a = 10\ \mu$m, $b = 50$ nm, $Q = 10^3$	4.2×10^{-12}

zone. A similar power enhancement can be achieved if an STNO is placed at the center of a nano-sized square capacitor (the length and the width of the capacitor plates are $a = 10\ \mu$m, and the distance between the plates is $b = 50$ nm). If we place an STNO in a rectangular waveguide or into a microstrip transmission line with the cross-section of $a \times b$, the electromagnetic field generated by an STNO can excite the fundamental propagating modes in these transmission lines. But this approach is less efficient ($P_{\text{dip}} \sim 10^{-14}$ W) than the previous one. In order to increase the emitted power, an STNO can be placed in a microwave resonator with a sufficiently high Q, which allows one to increase the emitted power by Q times [see Eq. (2)]. However, our calculations performed for a rectangular resonator (having a reasonably high quality factor $Q = 10^5$) demonstrated that the power emitted in such a resonator is smaller than the power that can be collected by a nano-loop. The power emitted into a resonator can be increased if the effective volume V_{eff} of the resonator is reduced. To achieve this, it is possible to place an STNO inside a parallel-plate resonator (the simplest model for a microstrip resonator) having the width a, height b, and length $l = \lambda/2$. For the reasonable sizes ($a = 10\ \mu$m, $b = 50$ nm) of the microstrip resonator, the emitted power equal to several pW can be obtained [19].

The calculations have demonstrated that the absolute values of microwave power emitted by a single STNO are rather small. Thus, to create a practical MSS based on STNOs, it would be useful to use arrays of coupled and synchronized STNOs [9, 11, 21]. There are two approaches to create such an array of STNOs. The first (traditional) approach

is to form an array of N oscillators connected in parallel or in series and coupled by a common bias current [23]. In such a case, the output power extracted through the MR mechanism from an array of N synchronized STNOs is N times larger than the power of a single STNO. The second approach is to place N STNOs (coupled through their dipolar electromagnetic fields) inside a resonator with a high Q-factor and to extract the power through the above-described dipolar emission mechanism. In that case, as it was shown in [24], the output power of the N-oscillator array can be N^2 times larger than the power of a single oscillator, whereas the total microwave power extracted from the resonator coupled to the array remains smaller than the power caused by the Gilbert damping in a single STNO in the array (typically this happens for $N \sim 10^4$).

Using the theory developed in [23] and assuming that a synchronized array of N STNOs is placed in a microstrip resonator, we can obtain the condition imposed on the number $N(f)$ of STNOs in the array, which guarantees that the microwave power extracted through the dipolar emission is larger than the power obtained through the MR mechanism [19]:

$$N(f) \geq N_{\text{c}} = \frac{P_{\text{MR}}}{P_{\text{dip}}(f)} = \frac{f_{\text{c}}^2}{f^2}. \tag{3}$$

Here, f_{c} is the characteristic frequency of the system (STNO + resonator), at which $P_{\text{dip}} = P_{\text{MR}}$ for a single STNO. The straight lines showing the dependence of the critical number of STNOs in an array N_{c} (3) on the generation frequency f for STNOs using the GMR (dashed red line) and TMR (solid blue line) effects are presented in Fig. 2. These lines were calculated for the case of STNOs coupled to a microstrip resonator
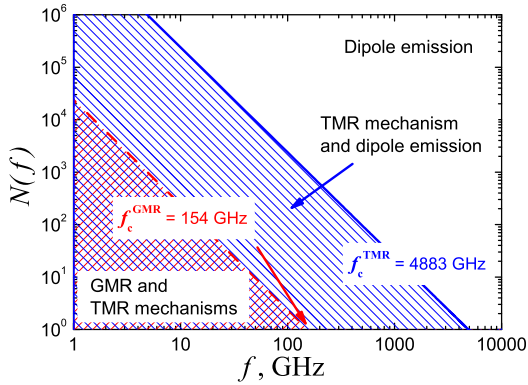
Fig. 2. Dependence of the critical number N_c (3) of STNOs in a synchronized array placed in a microstrip resonator on the generation frequency f. From [19]
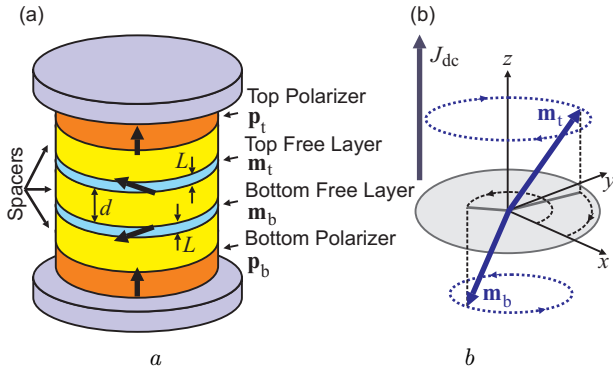

Fig. 3. (*a*) Layout of the symmetric dual-free-layer STNO consisting of four magnetic layers: two inner FLs of thickness L and two outer PLs separated by the GMR spacer of thickness d. (*b*) The torques acting on the magnetization vectors of the FLs in the STNO driven by the transverse bias dc current of the density J_{dc}

considered above, by assuming that $P_{MR} = 1$ nW for a GMR nano-oscillator and $P_{MR} = 1$ μW for a TMR nano-oscillator. The characteristic frequencies f_c in these two cases are $f_c^{GMR} \simeq 154$ GHz and $f_c^{TMR} \simeq 4.883$ THz, respectively. The regions above the GMR (dashed) and TMR (solid) lines are the regions, where the direct dipolar emission from a synchronized array of STNOs provides the larger output microwave power than the corresponding MR effects. Thus, the direct dipolar emission mechanism might become preferable as compared with the MR mechanism for sufficiently large arrays of coupled synchronized STNOs placed in a high-Q microwave resonator.

4. Microwave Sources Based on a Dual-Free-Layer Spin-Torque Nano-Oscillator

In order that MSSs based on STNOs become practical in modern microwave signal processing systems, it is necessary to enlarge the range of STNOs' operational frequencies, to improve their phase noise characteristics, and to increase their integrated output power [25, 26]. It is, also, preferable that these devices should be able to operate in a zero bias dc magnetic field. A step toward the development of such a practical STNO has been made in [10], where an oscillator with a perpendicular polarizer has been demonstrated. This type of STNO offers a significant improvement in the microwave power emission over conventional STNOs consisting of an in-plane FL and an in-plane PL. The main limitation of this structure, however, is a relatively low maximum frequency caused by the formation of a static vortex in the FL at high densities ($J_{dc} > J_v$) of the dc current [27].

Here, we consider a symmetric dual-free-layer (DFL) STNO containing two perpendicularly polarized PLs and two adjacent FLs with easy-plane anisotropy (Fig. 3, *a*). Such STNO could be used as a high-frequency MSS in the zero bias magnetic field, because it is possible in such a geometry to achieve the opposite directions of the current-driven magnetization precession in the FLs, and, therefore, to double the generated microwave frequency (the angle between the magnetizations of the FLs in a dual-free-layer STNO changes twice as fast as the angle between the magnetizations of the free and pinned layers) [28]. Below, we consider the regime of DFL nano-oscillator operation, when the FL magnetizations precess *in the opposite directions* along the large-angle out-of-plane trajectories and generate a relatively large microwave power at a frequency that is a sum of the magnetization precession frequencies in individual FLs. The power generated by a dual-free-layer STNO is several times higher than the power generated by a conventional STNO [29].

The considered STNO is a circular nano-pillar consisting of four metallic ferromagnetic layers separated by three non-magnetic spacers (see Fig. 3, *a*). The outermost magnetic layers serve as current polarizers and have magnetizations directed out of the sample plane along the *z*-axis of the coordinate system shown in Fig. 3, *b*; $\mathbf{p}_i = \hat{\mathbf{z}}$ are the unit vectors in the di-

rection of the magnetizations of the PLs, $i = $ t and $i = $ b for the top and bottom layers, respectively, $\hat{\mathbf{z}}$ is the unit vector of the z-axis. The magnetizations $\mathbf{M}_i$ of the two inner ferromagnetic layers lie in the plane of the sample at equilibrium, and these layers serve as the FLs of the STNO; $\mathbf{M}_i = M_0 \mathbf{m}_i$, $\mathbf{m}_i$ is the unit vector along the magnetization vector in the ith FL.

Although the layout of a dual-free-layer STNO contains four magnetic layers (see Fig. 3, *a*), we assume in the following that the magnetizations of the PLs are completely fixed and lie strictly perpendicularly to the layers' plane. Therefore, we consider only the STT-induced dynamics in the two FLs. We use the macrospin approximation to describe the magnetization dynamics in the FLs and also assume that the considered system operates in the zero bias dc magnetic field and is completely symmetric (the thicknesses and magnetic parameters of both FLs are the same). We consider a case where the FLs of the STNO are coupled with one another by the dipole-dipole interaction and are characterized by an easy-axis in-plane anisotropy. Despite the obvious limitations of the chosen model, it is sufficiently accurate in the case where the density J_{dc} of the bias dc current is lower ($J_{\mathrm{dc}} < J_{\mathrm{v}}$) than the density J_{v} corresponding to the vortex formation threshold calculated in [30]. Our model allows one to correctly predict the value of threshold J_{th} corresponding to the appearance of a stable dynamics determined from the much more complicated and time-consuming micromagnetic simulations [30]. It also satisfactorily describes the dependence of the generated microwave frequency $f(J_{\mathrm{dc}})$ on the density of the bias dc current J_{dc} for current densities below the threshold of vortex formation J_{v}.

The dynamics of the magnetizations in an STNO is governed by the normalized Landau–Lifshitz–Gilbert–Slonczewski (LLGS) equations written for the unit vectors $\mathbf{m}_i \equiv \mathbf{m}_i(t)$ [17, 18]:

$$\frac{d\mathbf{m}_i}{dt} = \gamma \left[\mathbf{B}_{\mathrm{eff},i} \times \mathbf{m}_i \right] + \alpha \left[\mathbf{m}_i \times \frac{d\mathbf{m}_i}{dt} \right] -$$
$$- \sigma_i J_{\mathrm{dc},i} \left[\mathbf{m}_i \times (\mathbf{m}_i \times \mathbf{p}_i) \right]. \qquad (4)$$

Here, the first term on the right-hand side of this equation is the conservative torque ($\mathbf{T}_P$), which induces the FLs' magnetizations to undergo the precession in opposite directions around the normal to

the sample plane [31] in the zero bias dc magnetic field (see Fig. 3, *b*). The second term is the dissipative Gilbert torque ($\mathbf{T}_D$) describing the energy dissipation, and the last term is the STT term ($\mathbf{T}_S$) describing the interaction of the magnetization with the spin-polarized current traversing the i-th FL. We used the following notations in (4): $\mathbf{B}_{\mathrm{eff},i}$ in the effective magnetic field acting on the i-th FL, σ_i is the "current density–torque" proportionality coefficient defined as [2]

$$\sigma_i = \frac{\gamma \hbar}{2 e M_0 L} \left[\frac{(1+\eta)^3}{4\eta^{3/2}} (3 + \mathbf{m}_i \mathbf{p}_i) - 4 \right]^{-1}, \qquad (5)$$

e is the modulus of the electron charge, and, finally, $J_{\mathrm{dc},i}$ is the bias dc current density traversing the STNO, which we specify as $J_{\mathrm{dc},i} = +J_{\mathrm{dc}}$ for the top FL ($i = $ t) and $J_{\mathrm{dc},i} = -J_{\mathrm{dc}}$ for the bottom layer ($i = $ b).

In our model, the field $\mathbf{B}_{\mathrm{eff},i}$ is written as

$$\mathbf{B}_{\mathrm{eff},i} = B_{\mathrm{A}} (\mathbf{m}_i \hat{\mathbf{x}}) \hat{\mathbf{x}} - \mu_0 M_0 (\mathbf{N}_{i,i} \mathbf{m}_i + \mathbf{N}_{i,j} \mathbf{m}_j), \qquad (6)$$

where $B_{\mathrm{A}} > 0$ is the magnitude of the anisotropy field [32] along the easy x-axis in both FLs, $\hat{\mathbf{x}}$ is the unit vector of the x-axis, $\mathbf{N}_{i,i}$ and $\mathbf{N}_{i,j}$ are the self-demagnetization and cross-demagnetization tensors [33], which depend on the self-demagnetization coefficient κ and the cross-demagnetization coefficient ρ, respectively. By turn, the dimensionless coefficients κ and ρ depend on the geometry of the structure [33].

For a quantitative description of the STNO's operation, we used the following typical parameters of the nano-pillar structure [30]: $R = 25$ nm, $L = 3$ nm, $d = 12$ nm, $\mu_0 M_0 = 704$ mT, $\eta = 0.3$. We simulated the dynamic behavior of our model system in a wide range of α values 0.002—0.09 and performed simulations, in which the field B_{A} was varied in the range 0—20 mT. In our case of the DFL nano-oscillator with chosen typical parameters $\kappa = 0.0707$, $\rho = 0.01134$.

Using the macrospin simulation procedure described in [29] in detail, we numerically solved the coupled LLGS equations (4) for the magnetizations of two FLs and calculated the frequencies of magnetization precession in the top (f_{t}) and bottom (f_{b}) FLs. The typical dependence of the frequency generated in a dual-free-layer STNO $f(J_{\mathrm{dc}}) \equiv f = f_{\mathrm{t}} + f_{\mathrm{b}}$
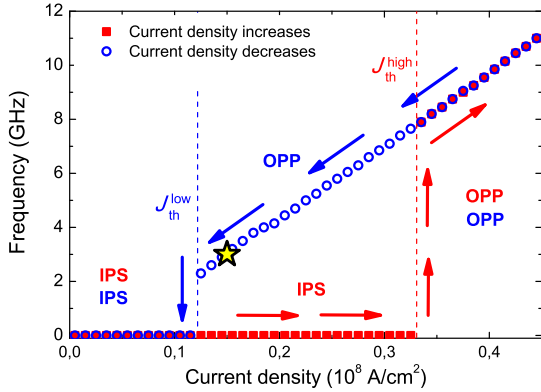
Fig. 4. Numerically calculated dependence of the frequency of an output signal f in a dual-free-layer STNO on the bias direct current density J_{dc}. The curves are calculated for $\alpha = 0.08$, $B_A = 5$ mT. From [29]

is shown in Fig. 4. As one can see, the frequency dependence on the bias current is different, by depending on whether the current density increases or decreases, i.e. this dependence demonstrates a strong hysteresis. When the density of the dc bias current is increased (red squares in Fig. 4), the magnetizations in both FLs stay in the in-plane static (IPS) state without any precession until the current density reaches a rather large magnitude J_{th}^{high} ($J_{th}^{high} \approx 0.33 \times 10^8$ A/cm^2 in Fig. 4). Above this critical (threshold) value, in the out-of-plane precessional (OOP) state, the magnetizations in both FLs start to precess in opposite directions, and the frequency of precession increases with the current density. Note that the generated frequency just above the threshold has a rather large value (about 8 GHz, see Fig. 4). However, when the density of the bias dc current is decreased (blue hollow points in Fig. 4), the regime of stable counter-precession of the FLs persists to rather low magnitudes of the bias current density J_{th}^{low} ($J_{th}^{low} \approx 0.12 \times 10^8$ A/cm^2 in Fig. 4), and the generated frequency, which decreases with a decrease of the current, can be much lower (down to approximately 2 GHz).

Note that the threshold value J_{th}^{high} (at which the stable counter-precession in two FLs starts) obtained in our macrospin simulations is very close to the threshold value $J_{th} \approx 0.35 \times 10^8$ A/cm^2 determined from the micromagnetic simulations [30]. This is a clear confirmation that our simplified "macrospin" model is sufficiently accurate to obtain even the quan-

titative information about the characteristics of a DFL nano-oscillator.

The origin of the hysteresis in a dual-free-layer STNO can be qualitatively explained as follows. In the absence of a bias dc current, the system exists in the IPS state. In this state, the magnetizations of the FLs are dipolarly coupled to each other, and the energy of the system is minimal, when the magnetizations have opposite directions. In other words, the dipolar coupling creates a potential well for the magnetizations (the in-plane anisotropy has a similar effect), and a finite torque (and, therefore, a finite bias current density J_{th}^{high}) is required to move the magnetizations out of this potential well. Thus, the higher threshold current J_{th}^{high} is determined by the depth of this potential well and depends, mainly, on the strength of the dipolar coupling between the FLs and/or on the strength of the in-plane anisotropy field. However, once the dipolar coupling between the two FLs is destroyed by a sufficiently strong spin torque created by the bias current, a much smaller spin torque is sufficient to sustain the persistent magnetization precession: as in the other types of STNO, the spin torque only needs to compensate the natural Gilbert damping in the FLs. Thus, the lower critical current J_{th}^{low} is determined by the energy losses and should be approximately proportional to the Gilbert damping constant α.

Using the numerical simulations [29] and analytical analysis [34], we found that the upper threshold J_{th}^{high} does not depend on the damping parameter α and is given by an approximate analytical expression $J_{th}^{high} = \rho \omega_M / \sigma_{eq}$, while the lower threshold J_{th}^{low} increases linearly with α (here, σ_{eq} is the equilibrium value of σ_i). This means that the upper current density threshold J_{th}^{high} can be controlled by choosing an appropriate geometry of the system corresponding to a certain particular value of parameter ρ. The other found interesting result is that the above-described hysteresis exists even in the absence of an in-plane anisotropy field. In that case, its existence is determined by the dipolar coupling between the FLs only.

The discovered hysteretic behavior of the dual-free-layer STNO yields the possibility of application of a strong initial pulse of the bias current (greater than the upper threshold of the stable dynamics J_{th}^{high}) and subsequent reduction of the bias current to a work-

ing point $J_{\text{th}}^{\text{low}} < J_{\text{dc}} < J_{\text{th}}^{\text{high}}$ corresponding to the required output frequency $f(J_{\text{dc}})$ [29].

5. Microwave Sources Based on a Vortex-State Spin-Torque Nano-Oscillator

It is well known that a flat magnetic element having a certain ratio of its thickness L to its in-plane size R in the absence of the external bias field reveals a vortex ground state [35]. When the vortex core is displaced from its equilibrium position at the center of the element, it starts to perform a damped gyrotropic rotational motion with a sub-gigahertz frequency [35]. When the damping of the gyrotropic mode (GM) is compensated by the STT [1, 2, 18], the self-sustained auto-oscillations involving the GM could be excited [36]. These auto-oscillations have an unusually narrow linewidth, and if a TMR nanopillar [37] is used instead of the GMR stack [36] and a moderate perpendicular bias field is applied, it is possible to substantially increase the output power of the gyrotropic vortex STNO, while preserving the narrow generation linewidth. Moreover, it was demonstrated that vortex-state auto-oscillators could be phase-locked to an external periodic signal [38] and synchronized between themselves [11], which makes these STNOs very promising for practical applications in the future nano-electronics.

Thus, it is tempting to use the general theory of nonlinear and non-isochronous auto-oscillators developed for regular (non-vortex) STNOs in [18] for the description of gyrotropic vortex STNOs and for the optimization of their working parameters. The main difficulty with this description was that, traditionally, the GM of the vortex motion was considered as an isolated mode – translational motion of a particle-like vortex core – and was described by a particular Thiele equation [35, 37, 39] for the motion of the vortex core. It was, however, shown in [40] that the GM can be treated as a regular SW mode in the framework of the standard Landau–Lifshitz description.

The standard framework for the theoretical description of the gyrotropic motion of the magnetic vortex core is the Thiele equation, which, in the presence of the STT, reads [37, 39, 41, 42]

$$\mathbf{G} \times \frac{d\mathbf{X}}{dt} + \frac{\partial W}{\partial \mathbf{X}} = \mathbf{F}_{\text{D}} + \mathbf{F}_{\text{ST}}. \tag{7}$$

Here, $\mathbf{X} = x\mathbf{e}_x + y\mathbf{e}_y$ is the two-dimensional position vector of the vortex core inside a magnetic disk of radius R, the gyrovector $\mathbf{G}$ has only the component $\mathbf{G} = G\hat{\mathbf{z}}$ perpendicular to the disk plane, and gyrovector magnitude is determined by the expression $G = (2\pi LM_0/\gamma)p_v$ ($p_v = \pm 1$ is the vortex core polarization), $W = W(\mathbf{X}, I_{\text{dc}})$ is the potential energy of the shifted vortex, $\mathbf{F}_{\text{D}} = -Gd_{\text{G}}(\mathbf{X})[\,d\mathbf{X}/dt\,]$, $\mathbf{F}_{\text{ST}} = G\sigma_{\text{G}}I_{\text{dc}}[\,\hat{\mathbf{z}} \times \mathbf{X}]$, $d_{\text{G}}(\mathbf{X})$ is the damping coefficient of the vortex core gyrotropic motion, which also depends on the vortex coordinate $\mathbf{X}$ [41, 42], $\sigma_{\text{G}} = (\sigma/2)p_v$, and σ is the spin-torque coefficient calculated for a non-vortex STNO (see Eq. (4b) in [18]). The vortex energy W arises from the presence of the demagnetization field related to the finite in-plane size of the magnetic disk and the presence of the transverse driving current I_{dc}. It is a nonlinear function of the vortex position $\mathbf{X}$, which can be developed in a Taylor series of powers of X^2 [41, 42].

In [43], we showed that the Thiele equation (7) can be rewritten in the form, which coincides exactly with the equation of the universal nonlinear auto-oscillator model (1) derived in [18], where the frequency and the positive and negative damping terms are expressed as: $\omega(p, I_{\text{dc}}) = 2G^{-1}R^{-2}[\partial W(p, I_{\text{dc}})/\partial p]$, $\Gamma_{+}(p, I_{\text{dc}}) = d_{\text{G}}(p)\omega(p, I_{\text{dc}})$, $\Gamma_{-}(p, I_{\text{dc}}) = \sigma_{\text{G}}I_{\text{dc}}$. Thus, if the nonlinear functions $W(p, I_{\text{dc}})$ and $d_{\text{G}}(p)$ are known, one can directly extend the auto-oscillator formalism developed in [18] to the case of a stable gyrotropic motion of a vortex core driven by STT.

The equilibrium (limit cycle) dimensionless auto-oscillation power p_0 of the GM can be determined from the energy balance condition: $\Gamma_{+}(p_0, I_{\text{dc}}) = \Gamma_{-}(I_{\text{dc}})$, while the non-isochronous parameters of a gyrotropic auto-oscillator, which determine its non-autonomous behavior near the limit cycle $p = p_0$, can be calculated as: $\Gamma_p(p_0, I_{\text{dc}}) = p_0[\partial\Gamma_{+}(p, I_{\text{dc}})/\partial p]$, $\nu(p_0, I) = (p_0/\Gamma_p)[\partial\omega/\partial p]$. Here, Γ_p is the damping parameter of small fluctuations from the equilibrium (limit cycle) power, and ν is the dimensionless parameter characterizing the auto-oscillator nonlinearity (see Eqs. (27b) and (33) in [18], respectively).

Using the general formalism described in [18] and the exact expressions obtained above, one can try to find the parameters Γ_p and ν of the gyrotropic STNO *directly from the experiment* using the fact that these parameters determine the frequency linewidths Δf_n of the n-th harmonic of the signal generated by a
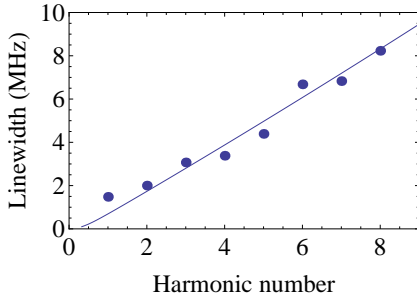
Fig. 5. Dependence of the harmonic linewidth Δf_n on the harmonic number n. Dots – experimental data, solid line – fit using Eqs. (8) and (9). From [43]

non-isochronous auto-oscillator [44]:

$$\Delta\phi^2(1/\Delta f_n) = 2\pi/n^2, \tag{8}$$

where $\Delta\phi^2(\tau)$ is the phase variance of the auto-oscillator (see Eq. (94b) in [18]):

$$\Delta\phi^2(\tau) = 2\pi\Delta f_1^{\text{iso}}\left[(1+\nu^2)|\tau| - \nu^2\frac{1 - e^{-2\Gamma_p|\tau|}}{2\Gamma_p}\right]. \tag{9}$$

Here, Δf_1^{iso} is the linewidth of the fundamental frequency harmonic ($n = 1$) in an isochronous ($\nu = 0$) auto-oscillator.

Thus, it follows from Eqs. (8) and (9) that it is necessary to measure experimentally the linewidths of at least three frequency harmonics of the generated signal to determine the parameters Γ_p, ν, and Δf_1^{iso} of a gyrotropic auto-oscillator.

We used the experimental data presented in Fig. 5 [43] and Eqs. (8), (9) to determine the parameters of a gyrotropic mode auto-oscillator. The solid line in Fig. 5 shows the fit of experimentally measured harmonic linewidths using Eqs. (8) and (9) with the following parameters: $\Delta f_1^{\text{iso}} = 12$ kHz, $\Gamma_p = 1.1 \times \times 10^6$ s^{-1}, and $\nu = 9$. One can see that the application of the standard theory of a non-isochronous auto-oscillator [18, 44] to a current-driven gyrotropic mode auto-oscillator provides a good explanation for the experimentally observed almost linear dependence of Δf_n on n, as opposed to the case of an isochronous auto-oscillator, where $\Delta f_n \sim n^2$.

6. Conclusions

We have demonstrated that, although the power of a single spin-torque nano-oscillator (STNO) obtained through the magnetoresistance effect is, in most cases, larger than the power of the direct dipolar emission from the same STNO, the latter mechanism might become preferable for sufficiently large arrays of coupled and synchronized STNOs placed in a high-Q microwave resonator.

We have reported that, in a microwave signal source (MSS) based on a dual-free-layer (DFL) STNO operating in the absence of the bias dc magnetic field, there is a strong hysteresis in the dependence of the frequency generated by the MSS on the bias dc current. When the bias current is increased, the microwave dynamics in the STNO starts at a relatively high value of bias current density. But when the bias current is decreased, this dynamics persists to a much lower value of bias current density. The lower threshold current is determined by the Gilbert damping parameter (precessional state vanishes due to the damping), while the higher threshold in the bias current is mainly caused by the existence of the in-plane anisotropy and the dipolar coupling between the FLs.

Finally, we have demonstrated that the previously developed theory of non-isochronous auto-oscillators [18] can be successfully applied to quantitatively describe the dynamic behavior of vortex-state STNOs and the corresponding MSSs. We also have shown that a vortex STNO could be strongly non-isochronous, demonstrating the almost linear dependence of the higher harmonic linewidths on the harmonic number.

1. L. Berger, Phys. Rev. B **54**, 9353 (1996).
2. J.C. Slonczewski, J. Magn. Magn. Mat. **159**, L1 (1996).
3. J.A. Katine, F.J. Albert, R.A. Buhrman *et al.*, Phys. Rev. Lett. **84**, 3149 (2000).
4. M. Tsoi, A.M.G. Jansen, J. Bass *et al.*, Phys. Rev. Lett. **80**, 4281 (1998).
5. S.I. Kiselev, J.C. Sankey, I.N. Krivorotov *et al.*, Nat. **425**, 380 (2003).
6. S. Kaka, M.R. Pufall, W.H. Rippard *et al.*, Nat. **437**, 389 (2005).
7. K.J. Lee, A. Deac, O. Redon *et al.*, Nat. Mater. **3**, 877 (2004).
8. I.N. Krivorotov, N.C. Emley, J.C. Sankey *et al.*, Sci. **307**, 228 (2005).

9. F.B. Mancoff, N.D. Rizzo, B.N. Engel, and S. Tehrani, Nat. **437**, 393 (2005).

10. D. Houssameddine, U. Ebels, B. Delaët *et al.*, Nat. Mater. **6**, 447 (2007).

11. A. Ruotolo, V. Cros, B. Georges *et al.*, Nat. Nanotech. **4**, 528 (2009).

12. A.A. Tulapurkar, Y. Suzuki, A. Fukushima *et al.*, Nat. **438**, 339 (2005).

13. O.V. Prokopenko *et al.*, in *Magnonics: From Fundamentals to Applications. Topics in Applied Physics*, edited by S.O. Demokritov and A.N. Slavin (Springer, Berlin, 2013).

14. J.C. Sankey, Y. Cui, J.Z. Sun, J.C. Slonczewski, R.A. Buhrman, and D.C. Ralph, Nature Phys. **4**, 67 (2008).

15. D.C. Ralph and M.D. Stiles, J. Magn. Magn. Mater. **320**, 1190 (2008).

16. A.M. Pogorilyi, S.M. Ryabchenko, and O.I. Tovstolytkin, Ukr. Fiz. Zh. Oglyady **6**, 37 (2010).

17. *Handbook of Spin Transport and Magnetism*, edited by E.Y. Tsymbal and I. Žutić (CRC Press, New York, 2012).

18. A. Slavin and V. Tiberkevich, IEEE Trans. Magn. **45**, 1875 (2009).

19. O. Prokopenko, E. Bankowski, T. Meitzler *et al.*, IEEE Magn. Lett. **2**, 3000104 (2011).

20. N. Amin, H. Xi, and M.X. Tang, IEEE Trans. Magn. **45**, 4183 (2009).

21. V. Tiberkevich, A. Slavin, E. Bankowski, and G. Gerhart, Appl. Phys. Lett. **95**, 262505 (2009).

22. S. Ramo, J.R. Whinnery, and T. van Duzer, *Fields and Waves in Communication Electronics* (Wiley, New York, 1984).

23. B. Georges, J. Grollier, V. Cross, and A. Fert, Appl. Phys. Lett. **92**, 232504 (2008).

24. A. Pikovsky, M. Rosenblum, and J. Kurths, *Synchronization: a Universal Concept in Nonlinear Sciences* (Cambridge Univ. Press, Cambridge, 2007).

25. J.A. Katine and E.E. Fullerton, J. Magn. Magn. Mater. **320**, 1217 (2008).

26. P.M. Braganca, B.A. Gurney, B.A. Wilson *et al.*, Nanotech. **21**, 235202 (2010).

27. I. Firastrau, D. Gusakova, D. Houssameddine *et al.*, Phys. Rev. B **78**, 024437 (2008).

28. G. Rowlands and I. Krivorotov, Abstracts of the 2009 APS March Meeting, BAPS.2009.MAR.W29.7, Pittsburgh, PA (2009).

29. O.V. Prokopenko, I.N. Krivorotov, E.N. Bankowski *et al.*, J. Appl. Phys. **114**, 173904 (2013).

30. G.E. Rowlands, and I.N. Krivorotov, Phys. Rev. B **86**, 094425 (2012).

31. A.D. Kent, B. Özyilmaz, and E. del Barco, Appl. Phys. Lett. **84**, 3897 (2004).

32. A.G. Gurevich and G.A. Melkov, *Magnetization Oscillations and Waves* (CRC Press, New York, 1996).

33. O. Dmytriiev, T. Meitzler, E. Bankowski *et al.*, J. Phys.: Condens. Matter **22**, 136001 (2010).

34. O.V. Prokopenko, V.S. Tiberkevich and A.N. Slavin, Funct. Mater. **21**, 206 (2014).

35. K.Y. Guslienko, J. Nanosci. Nanotechn. **8**, 2745 (2008).

36. V.S. Pribiag, I.N. Krivorotov, G.D. Fuchs *et al.*, Nat. Phys. **3**, 498 (2007).

37. A. Dussaux, B. Georges, J. Grollier *et al.*, Nat. Commun. **1**, 8 (2010).

38. A. Dussaux, A.V. Khvalkovskiy, J. Grollier *et al.*, Appl. Phys. Lett. **98**, 132506 (2011).

39. A.A. Thiele, Phys. Rev. Lett. **30**, 230 (1973).

40. K.Y. Guslienko, A.N. Slavin, V. Tiberkevich, and S.K. Kim, Phys. Rev. Lett. **101**, 247203 (2008).

41. K.Y. Guslienko, G.R. Aranda, and J. Gonzalez, J. Phys.: Conf. Ser. **292**, 12006 (2011).

42. A. Dussaux, A.V. Khvalkovskiy, P. Bortolotti *et al.*, Phys. Rev. B **86**, 014402 (2012).

43. F. Sanches, V. Tiberkevich, K.Y. Guslienko *et al.*, Phys. Rev. B. **89**, 140410(R) (2014).

44. M. Quinsat, V. Tiberkevich, D. Gusakova *et al.*, Phys. Rev. B **86**, 104418 (2012).

О.В. Прокопенко

ДЖЕРЕЛА МІКРОХВИЛЬОВИХ
СИГНАЛІВ НА ОСНОВІ СПІНТРОННИХ
МАГНІТНИХ НАНООСЦИЛЯТОРІВ

Р е з ю м е

Ефект переносу спінового моменту обертання електричним струмом (STT) є новим методом впливу на намагніченість нанооб'єктів. Цей метод дозволяє збудити мікрохвильові коливання намагніченості у шаруватих спінтронних наноструктурах, пропускаючи крізь них електричний струм, що може бути використане для розробки мікрохвильових джерел сигналів (МДС). У роботі розглянуто основні результати щодо МДС, заснованих на STT ефекті, отримані у Київському національному університеті імені Тараса Шевченка та закордонних партнерських установах за останні декілька років.